Magn Reson Med Sci 2017; 16; 190–202
doi:10.2463/mrms.mp.2016-0051
Published Online: November 4, 2016

MAJOR PAPER

Application of Cardiac Gating to Improve the Reproducibility of Intravoxel Incoherent Motion Measurements in the Head and Neck

Koung Mi Kang[1,2], Seung Hong Choi[1-4*], Dong Eun Kim[5], Tae Jin Yun[1,2], Ji-hoon Kim[1,2], Chul-Ho Sohn[1-3], and Sun-Won Park[6]

Purpose: To prospectively evaluate whether cardiac gating can improve the reproducibility of intravoxel incoherent motion (IVIM) parameters in the head and neck, we performed IVIM diffusion-weighted imaging (DWI) using 4 b values (4b), 4 b values with cardiac gating (4b gating) and 17 b values (17b).

Methods: We performed IVIM DWI twice per person on nine healthy volunteers using 4b, 4b gating and 17b and five patients with head and neck masses using 4b gating and 17b. The ADC, perfusion fraction (*f*), diffusion coefficient (D) and perfusion-related diffusion coefficient (D*) were calculated in the brain, masticator muscle, parotid gland, submandibular gland, tonsil and masses. Intraclass coefficient (ICC), Bland-Altman analysis (BAA) and coefficient of variation (CV) were used to assess short-term test-retest reproducibility. Kruskal-Wallis test and Mann-Whitney test were used to investigate whether 4b, 4b gating or 17b had significant influences on the parameters.

Results: For normal tissues and masses, ICC was excellent for all maps except the D* map. All parameters showed the lowest CV in the 4b gating. BAA also revealed the narrowest 95% limits of agreement using 4b gating for all parameters. In the subgroup analysis, almost all parameters in brain, muscle, parotid gland and submandibular gland showed the best reproducibility using 4b gating. In the muscle, parotid gland and submandibular gland, the values of ADC, *f* and D were not significantly different between among the three methods.

Conclusion: 4b gating was more reproducible with respect to measurements of IVIM parameters in comparison with 4b or 17b.

Keywords: *intravoxel incoherent motion, diffusion weighted imaging, head and neck, reproducibility, cardiac gating*

Introduction

Recently, intravoxel incoherent motion (IVIM) theory has been an active area of research with regard to head and neck masses as a non-contrast enhanced perfusion and diffusion MR imaging technique.[1–5] Because IVIM analysis can separate the effects of diffusion and perfusion,[6] previous studies in the head and neck have demonstrated that IVIM parameters are important biomarkers. For example, IVIM parameters can be used as predictive indicators of tumor staging of nasopharyngeal carcinomas,[7] therapy monitoring,[4] and prediction of treatment outcomes.[8]

An important part of the IVIM diffusion-weighted imaging (DWI) acquisition is the choice of b values, which control the intensity of the bipolar gradient pulses and define the degree of diffusion weighting in the acquired signal.[9] Thus far, there is no consensus on the number and magnitude of b values that should be applied for clinical measurements. The number of b values used for IVIM DWI varies among studies and ranges from 4 to more than 10.[10] Four is the minimum number of b values to characterize biexponential signal attenuation for four fitted parameters. Although using more b values has been predicted to provide more support for the estimates and correct the fitting error of a biexponential curve, there is a time limitation related to acquiring images. In addition, a large number of b values can make the scan vulnerable to motion artifacts.

[1]Department of Radiology, Seoul National University Hospital, 101 Daehak-ro, Jongno-gu, Seoul 110-744, Korea
[2]Department of Radiology, Seoul National University College of Medicine, Seoul, Korea
[3]Center for Nanoparticle Research, Institute for Basic Science (IBS), Seoul, Korea
[4]School of Chemical and Biological Engineering, Seoul National University, Seoul, Korea
[5]General Electronics (GE) Healthcare Korea, Seoul, Korea
[6]Department of Radiology, Seoul National University Boramae Hospital, Seoul, Korea

*Corresponding author, Phone: +82-2-2072-2584, Fax: +82-2-747-7418, E-mail: verocay@snuh.org

Received: March 16, 2016 | Accepted: September 9, 2016

Optimization of a protocol and a robust estimation of diffusion and perfusion properties are important for achieving the best diagnostic performance of IVIM DWI. However, there is limited knowledge on the reproducibility of IVIM parameters in the head and neck. Furthermore, there are very limited data regarding the performance of the minimum, four b values, with respect to acquiring appropriate IVIM parameters compared with greater numbers of b values. Due to limited acquisition time, an evaluation of IVIM DWI that uses the minimum number of b values should be compared with processes that use more than 10 b values. The number of b values is not the only relevant parameter. As previous studies have reported, the value of IVIM parameters is dependent on the cardiac cycle.[11–13] There are also pulsatile flow in the head and neck, which is caused by neck vessels and CSF in the spinal canal. In addition, the flow can affect the results through partial volume effects. We presumed that cardiac gating might be helpful in improving IVIM acquisition.

Therefore, the objective of this study was to prospectively evaluate whether cardiac gating can improve the reproducibility of the ADC and IVIM parameters in the head and neck; to achieve this, we performed IVIM DWI using 4b values (4b), 4b values with cardiac gating (4b gating) and 17b values (17b).

Materials and Methods

Our institutional review board approved this prospective study protocol. Signed informed consent was obtained from all volunteers.

Study population

Nine healthy volunteers (mean age, 32 years; age range, 25–51 years; five men [mean age, 34 years; age range, 27–51 years], four women [mean age, 30 years; age range, 25–40 years]) were enrolled in the study from August 2014 to October 2014. Inclusion criteria for healthy volunteers were as follows: volunteers with no artificial dental material or only one MRI compatible dental material that produces no detectable distortions on MRI.[14]

We acquired IVIM imaging from the consecutive patients who had head and neck masses on the previous MRI.

The patients underwent additional IVIM imaging on the follow-up MR examinations which were taken from July 2015 to August 2015. We excluded a patient who showed significant susceptibility artifact on the MRI. In addition, a patient was excluded because his neck mass disappeared on the follow-up MRI. Finally, five patients (mean age, 51 years; age range, 22–78 years; two mean [22 years and 63 years, respectively] and three women [37 years, 53 years and 78 years, respectively]) were enrolled in the study. Six masses from five patients were included in this study. A patient with a glomus vagale paraganglioma underwent endovascular embolization 7 years ago and radiotherapy 6 years ago. A patient with bilateral level II metastatic lymph nodes from sinonasal adenocarcinoma underwent radiotherapy 2 months ago. Three patients with neurogenic tumors were in follow-up without treatment.

MR examination

All the examinations were performed by a 1.5T scanner (Signa HDxt, GE Healthcare, WI, USA) with an 8-channel head and neck coil (1.5T 8 Channel Medrad Neurovascular Array, general electronics Healthcare). DWI were acquired twice with a single-shot EPI pulse sequence using four different b values (b = 0, 200, 400, and 800 s/mm^2) with and without peripheral cardiac gating and 17 b values (b = 0, 10, 15, 20, 25, 30, 50, 80, 100, 120, 140, 160, 200, 300, 500, 800, and 1000 s/mm^2). Because both low b values (≤200 s/mm^2) and high b values (>200 s/mm^2) were needed to gain both perfusion and diffusion related information, the 4b and 4b gating consisted of 0, 200, 400 and 800 s/mm^2. The distribution and values of the 17b setup were similar to the previously reported distribution of 16b values.[15–17] Cardiac gating allowed for stop motion imaging by acquiring data only during a specified portion of the cardiac cycle, typically during diastole when the heart is not moving.

The IVIM DWI set consisted of 4b, 4b gating and 17b and was performed twice in all volunteers. Images were obtained in the following order: The first 4b, the first 4b gating, the first 17b, the second 4b, the second 4b gating and the second 17b. For patients, the MRI DWI set of 4b gating and 17b was obtained twice; the first 4b gating, the first 17b, the second 4b gating and the second 17b. The bed of the MR machine was pulled and pushed after the first scan. The time intervals between obtaining the first and second IVIM DWI with the same conditions were approximately 14 minutes in the volunteers and 10 minutes in the patients, respectively. To avoid motion artifact resulted from swallowing, volunteers and patients were asked to reduce swallowing during the scans. MR parameters for each scan are described in Table 1. We obtained all DWI with the same FOV, slice thickness, and matrix. For

Table 1. IVIM DW MR imaging parameters

Parameter	4b	4b gating	17b
b values (s/mm^2)	4	4	17
Gating	No	Yes	No
TR (msec)/TE (msec)	7000/64.2	9800 ± 1000/64.2	7300/67.1
Bandwidth (khz)	250	250	250
FOV (mm)	240*240	240*240	240*240
Slice thickness (mm)/slice gap (mm)	4/1.2	4/1.2	4/1.2
Matrix	128*96	128*96	128*96
Number of average (b = 0)	4	4	4
Number of average (b = others)	2	2	1
Frequency direction	Right/Left	Right/Left	Right/Left
Acquisition time (min:sec)	02:41	03:46	07:33

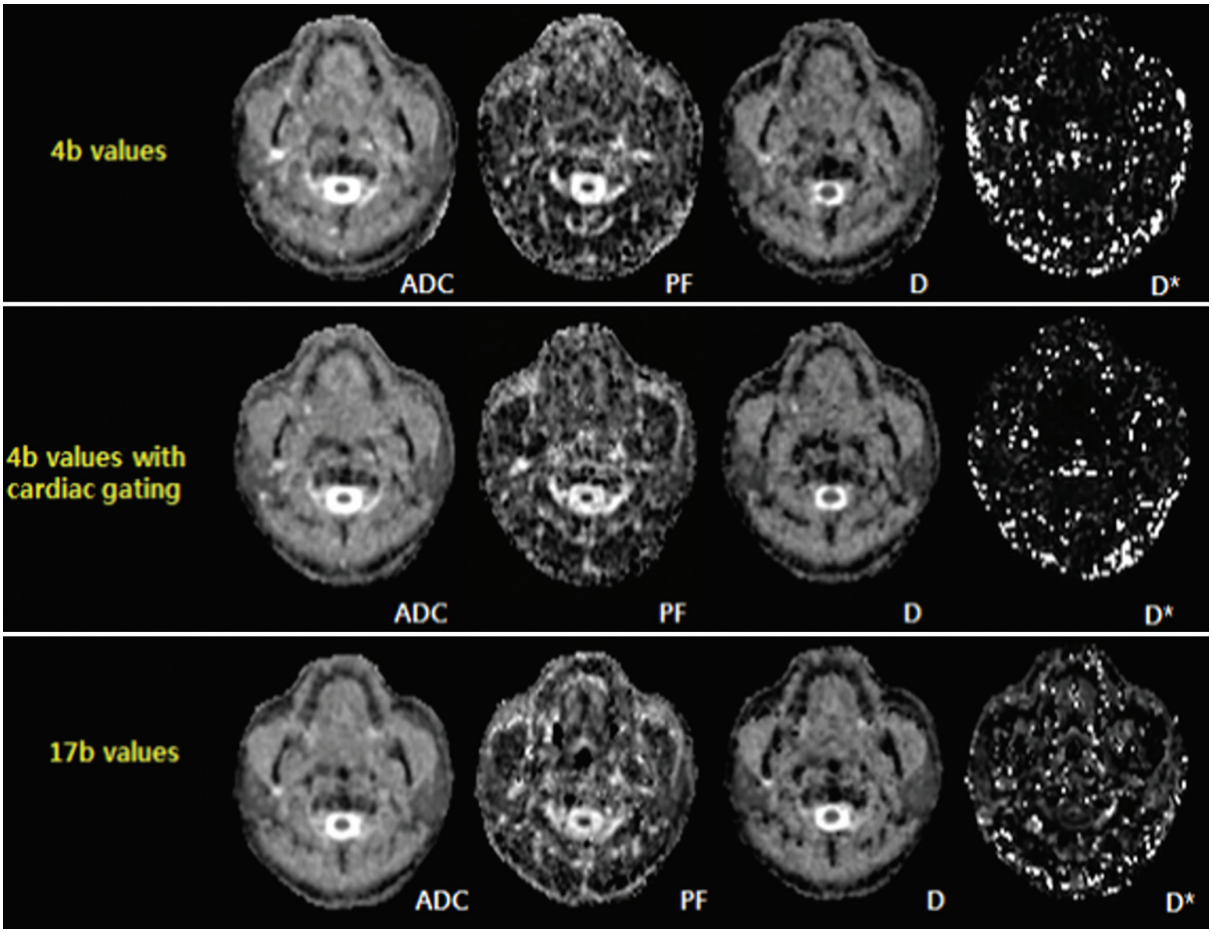

Fig 1. Representative maps of ADC and IVIM parameters using 4 b values, 4b values with cardiac gating and 17 b values in a 50-year-old male volunteer.

TR and TE, we obtained slightly different values due to cardiac gating and the number of b values. To reduce the susceptibility to artifacts in EPI and maximize the signal to noise ratio of DWI, the ASSET parallel imaging technique and numbers of excitations with a factor of two were used, respectively. DW image was acquired with three directional diffusion gradients and then combined into one (Slice (0,0,1), Readout (1,0,0), Phase Encoding (0,1,0)). The combined DW image was used for IVIM fitting. The ADC was calculated by fitting all b values to the following equation: $S_b = S_0 \exp(-ADC * b)$, where S_b is the signal intensity at a given b value and S_0 is the signal intensity observed in the absence of a diffusion gradient. Representative images in a volunteer and a patient are illustrated in Figs. 1 and 2, respectively.

Image analysis

The acquired DW images were analyzed using an IVIM model to measure both molecular diffusion and tissue perfusion parameters. The DW signal intensity decay with b values can be expressed by the following biexponential function[6]:

$$S_b / S_0 = (1 - f) \cdot \exp(-bD) + f \cdot \exp[-b(D + D^*)]$$

Where f is the perfusion fraction (in %), D is the diffusion coefficient (in mm^2/s) and D* is the perfusion-related diffusion coefficient (in mm^2/s). IVIM post-processing was programmed using Matlab (The Mathworks Inc., Natick, MA, USA). The fitting procedure was performed to generate maps of f, D, D* using non-linear least square fitting with three unknowns, Lvenberg-Marquardt (MATLAB, Mathworks Inc., Natick, MA). Gaussian smoothing with a spatial kernel of 3 × 3 × 3 was used for IVIM fitting.

Quantitative analysis of IVIM DWI was performed by a radiologist (K.M.K, 6 years of experience in the head and neck imaging). In the volunteers, free-hand ROIs were drawn on the maps of ADC and IVIM parameters including f, D and D* to cover the brain (i.e., pons, cerebellum), bilateral masticator muscles, bilateral parotid glands, bilateral submandibular glands and bilateral tonsils. In the patients, free-hand ROIs were drawn to encompass the nearly entire masses in each patient. The ROI was placed in the most representative slice of each anatomical region to avoid unrealistic value. All ROIs were directly co-localized on all parameter maps. Values of ADC, f, D and D* were calculated from the averaged signal of the ROIs.

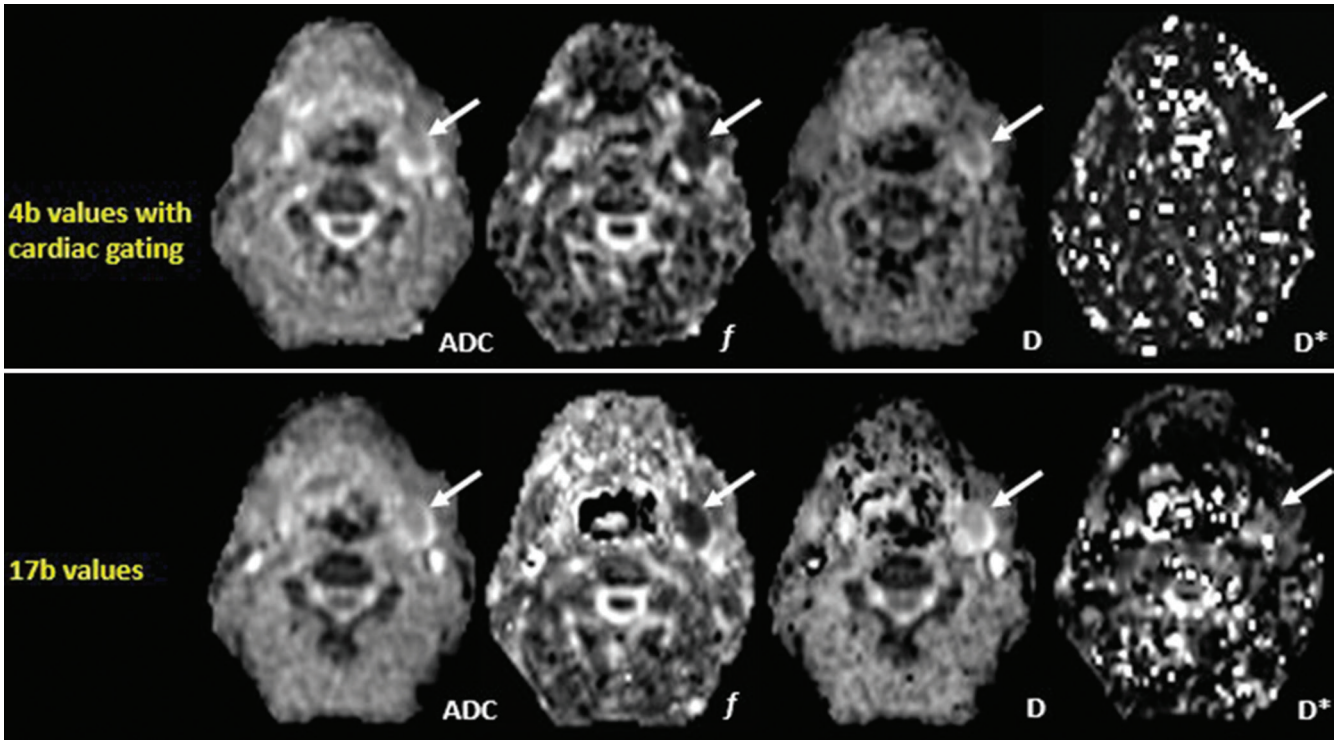

Fig 2. Representative maps of ADC and IVIM parameters using 4b values with cardiac gating and 17 b values in a 63-year-old male patient with a neurogenic tumor in the left level II (arrow).

Statistical Analysis

Most recent studies which evaluated reproducibility used the combination of the intraclass coefficient (ICC), Bland-Altman analysis (BAA), and the coefficient of variation (CV) as statistical methods.[18–22] Therefore, we compared short-term test-retest reproducibility between IVIM DW images using the 4b, 4b gating and 17b methods using ICC, CV and BAA. Two types of subgroup analyses were also performed to ADC and IVIM parameters in various tissues in the head and neck. Among the various guidelines for the interpretation of the ICC, we adapted a scale introduced in previous research: ICC values less than 0.40 indicate poor reproducibility, ICC values of 0.40–0.75 indicate fair-to-good reproducibility, and ICC values greater than 0.75 indicate excellent reproducibility.[23] We performed a BAA, which yielded the mean difference and the 95% limits of agreement between short-term test-retest results (expressed as a percentage). CV values were calculated as follows: the standard deviation was divided by the mean, and the result was presented as a percentage (100 × standard deviation/mean).[24] Higher ICC values, lower CV values and narrower 95% limits of agreement indicated better short-term test-retest reproducibility.

The Kolmogorov-Smirnov test was used to determine whether the values of ADC and IVIM parameters were normally distributed ($P < 0.05$ indicates non-normal distribution). We used the mean values of short-term test-retest measurements to define the measured parameters. The results were reported as median values with ranges in parentheses. The Kruskal-Wallis test followed by post-hoc analyses was used to compare ADC and IVIM parameters between 4b, 4b gating and 17b in each normal anatomical region and to compare the values of ADC and IVIM parameters between different anatomical regions in each setting. The Mann-Whitney test was used to compare the values of ADC and IVIM parameters between 4b gating and 17b in the patients group. A *P*-value of less than 0.05 was considered an indication of statistical significance. Commercially available software (MedCalc, version 11.1.1.0, MedCalc software, Mariakerke, Belgium) was used for the analysis.

Results

Short-term test-retest reproducibility of ADC and IVIM parameters in normal head and neck tissues

All nine subjects underwent the IVIM DWI set twice. ROIs were acquired in 9 pons, 9 cerebella, 18 masticator muscles, 18 parotid glands, 18 submandibular glands and 16 tonsils. In the two left tonsils, ROI placement was not possible due to poor image quality caused by the small size of the tonsils and susceptibility artifacts around the airway. The size of ROI (mean ± standard deviation) was as follows; 92.8 ± 42.6 mm^2 for pons, 220.2 ± 52.0 mm^2 for cerebellum, 104.3 ± 41.6 mm^2 for masticator muscle, 80.8 ± 36.7 mm^2 for parotid gland, 65.2 ± 31.8 mm^2 for submandibular gland

Table 2. Short-term test-retest reproducibility of ADC and IVIM parameters in normal head and neck tissues

		4b	4b gating	17b
ICC[a]	ADC	0.974 (0.961 – 0.983)	0.985 (0.977 – 0.990)	0.978 (0.966 – 0.989)
	f	0.794 (0.685 – 0.865)	0.838 (0.753 – 0.894)	0.592 (0.378 – 0.733)
	D	0.954 (0.930 – 0.970)	0.971 (0.955 – 0.981)	0.959 (0.938 – 0.973)
	D*	0.264 (–0.123 – 0.518)	0.303 (–0.064 – 0.544)	0.319 (–0.340 – 0.554)
CV[b]	ADC	4.76	3.74	4.49
	f	20.45	15.27	22.14
	D	7.48	5.67	8.19
	D*	38.74	29.24	41.80
BAA[c]	ADC	–0.9 (–23.6, 21.7)	–1.0 (–17.2, 15.1)	0.1 (–19.9, 30.0)
	f	1.1 (–73.6, 75.9)	2.8 (–58.0, 63.6)	–6.2 (–89.5, 77.1)
	D	0.5 (–33.4, 34.3)	–2.2 (–28.0, 23.5)	2.2 (–38.1, 42.4)
	D*	13.8 (–127.3, 154.9)	–0.4 (–105.2, 104.4)	7.4 (–138.4, 153.2)

All numbers in brackets of [a]ICC indicate the 95% confidence interval. The highest ICC value indicates the best reproducibility. The lowest mean of [b]CV (in %) indicates the best reproducibility. Mean difference and 95% limits of agreement [c]BAA (in %) are shown. The narrowest value indicates the best reproducibility.

Table 3. Mean CV (%) of ADC and IVIM parameters on repeated IVIM DW images

		4b	4b gating	17b
Brain	ADC	4.44	1.21*	1.25
	f	12.7	8.62*	10.57
	D	2.7	1.31*	1.4
	D*	24.8	19.56*	33.43
Muscle	ADC	2.14*	2.29	3.52
	f	27.6	17.3*	20.88
	D	3.29	3.24*	4.25
	D*	48.03	32.28*	33.68
Parotid	ADC	3.96	2.23*	2.69
	f	16.67	6.88*	14.4
	D	7.44	4.28*	5.88
	D*	30.68	24.19*	31.01
Submandibular glands	ADC	4.81	4.51*	4.47
	f	19.78	12.14*	26.5
	D	10.46	5.94*	7.59
	D*	49.87	33.44*	46.33
Tonsil	ADC	8.92*	9.08	11.28
	f	26.09*	33.37	40.37
	D	14.27*	15.16	23.54
	D*	40.5	37.67*	67.37

*The lowest value indicates the best reproducibility.

and 18.7 ± 4.2 mm^2 for tonsil., ICC values of ADC, *f* and D were excellent and the highest using 4b gating technique (Table 2). For D*, ICC values indicated poor reproducibility in all trials.

For individual parameters, all parameters presented the lowest mean CV using the 4b gating (Table 2). CV values in the subgroup analysis in various tissues in the head and neck are described in Table 3. Among the techniques (i.e., 4b, 4b gating and 17b), the brain, parotid gland and submandibular glands exhibited the lowest mean CV using 4b gating for ADC and all IVIM parameters. In the muscles, all parameters except ADC, that is, all IVIM parameters, presented the lowest CV using 4b gating. In the tonsils, all parameters except D* exhibited the lowest CV value using 4b, and D* presented the lowest CV value using 4b gating.

Regarding individual parameters, Bland-Altman analyses revealed the narrowest 95% limits of agreement in all parameters using 4b gating (Table 2). Regarding the subgroup analysis in various tissues in the head and neck, mean differences and 95% limits of agreement of repeated IVIM DWI are described in Table 4. In the muscle, parotid gland and submandibular glands (i.e., all tissues except the tonsils and brain), all parameters revealed narrower 95% limits of agreement using 4b gating than 4b or 17b. In the brain, all parameters except D showed narrower 95% limits of agreement using 4b gating than 4b or 17b. In the tonsils, D and D* exhibited the narrowest 95% limits of agreement using 4b gating whereas ADC and *f* showed exhibited the narrowest 95% limits of agreement using 4b.

In general, D* exhibited the worst 95% limits of agreement with respect to short-term measurement reproducibility for all parameters regardless of the tissue and the number of b value

Table 4. Mean difference and 95% limits of agreement for ADC and IVIM parameters on repeated IVIM DW images

		4b	4b gating	17b
Brain	ADC	–3.3 (–28.5, 21.9)	–0.4 (–5.1, 4.3)*	–0.6 (–5.7, 4.5)
	f	5.5 (–43.1, 53.5)	2.2 (–28.5, 33.0)*	1.0 (–35.1, 37.1)
	D	–0.8 (–11.6, 10.0)	–0.6 (–5.8, 4.6)	–0.7 (–5.5, 4.3)*
	D*	2.6 (–117.6, 122.8)	19.4 (–54.2, 93.0)*	–1.8 (–118.4, 114.5)
Muscle	ADC	–0.3 (–9.0, 8.3)	0 (–8.2, 8.2)*	–1.5 (–15.3, 12.4)
	f	4.3 (–97.6, 106.2)	–4.3 (–59.6, 51.0)*	–7.5 (–90.3, 75.3)
	D	–0.9 (–14.2, 12.5)	0.2 (–10.2, 10.6)*	–2.0 (–17.9, 14.0)
	D*	11.1 (–157.7, 179.9)	–30.2 (–134.3, 73.8)*	–8.9 (–134.3, 116.4)
Parotid	ADC	2.6 (–11.3, 16.5)	0 (–8.1, 8.1)*	0.3 (–10.5, 11.0)
	f	–1.3 (–54.1, 51.5)	3.6 (–19.2, 26.4)*	–2.1 (–53.8, 49.7)
	D	2.6 (–23.1, 28.4)	1.1 (–17.9, 20.1)*	1.5 (–22.8, 25.8)
	D*	2.7 (–114.5, 119.9)	–1.6 (–81.1, 77.8)*	9.1 (–96.6, 114.8)
Submandibular glands	ADC	0.2 (–27.2, 27.6)	–1.8 (–18.3, 14.6)*	0.5 (–16.0, 16.9)*
	f	3.2 (–68.4, 74.7)	–5.7 (–49.9, 38.5)*	–2.3 (–93.6, 89)
	D	–1.6 (–50.7, 47.5)	–1.8 (–21.5, 17.8)*	–1.4 (–31.8, 29.1)
	D*	29.1 (–129.7, 187.9)	14.6 (–88.5, 117.6)*	–0.6 (–161.1, 160.0)
Tonsil	ADC	–4.3 (–35.2, 26.6)*	–3.2 (–34.9, 28.5)	2.0 (–37.9, 42.0)
	f	–6.7 (–99.4, 86.1)*	20.0 (–91.1, 131.1)	–21.7 (–152.7, 109.2)
	D	3.3 (–49.2, 55.8)	–10.9 (–60.4, 38.6)*	14.7 (–66.3, 95.7)
	D*	24.7 (–116.2, 165.6)	–4.4 (–142.6, 133.8)*	43.0 (–159.9, 245.9)

Data in parentheses are 95% limits of agreement (%). * The narrowest value indicates the best reproducibility.

compared with other parameters. An example of test-retest fitted curve in the normal head and neck tissues is in Fig. 3.

The Kruskal-Wallis test revealed that all parameters except D* exhibited no statistically significant difference among the three methods in the muscle, parotid gland and submandibular glands (All $P > 0.05$ for ADC, D and *f*, $P = 0.0002$, $P < 0.0001$, and $P = 0.003$ for D*). In the post hoc analysis for D*, there were significant differences in 4b gating vs 4b and 4b gating vs 17b in muscle, 17b vs 4b and 17b vs 4b gating in the parotid gland, and 4b gating vs 17b in the submandibular glands.

In the brain, all parameters except *f* revealed no statistically significant differences among the three methods (i.e., all $P > 0.05$ for ADC, D and D*; $P = 0.014$ for *f*). In the post hoc analysis of *f* in the brain, there was a significant difference between 4b and 17b.

In the tonsils, the diffusion related parameters, ADC and D, exhibited no statistically significant differences among the three methods ($P = 0.089$ for ADC, $P = 0.466$ for D). On the other hand, the perfusion related parameters, *f* and D*, revealed statistically significant differences among the three methods in the tonsils ($P = 0.033$ for *f*, $P < 0.0001$ for D*). In the post-hoc analysis of the tonsils, there was a significant difference in 4b gating vs 17b for *f*, and 17b vs 4b and 17b vs 4b gating for D*. Fitted curves comparing 4b, 4b gating and 17b in the normal head and neck tissues of a case are seen in Fig. 4.

ADC and IVIM parameters in the different anatomical regions of normal head and neck tissues

Median values and ranges of the mean values of ADC, *f*, D, and D* calculated from short-term test-retest IVIM DWI are described in Table 5.

The results of Kruskal-Wallis test are described in Table 6. Regarding ADC value, all anatomical regions showed significantly different values in 4b, 4b gating and 17b. Muscle revealed the highest ADC value, followed by submandibular gland, parotid gland, tonsil and brain. For *f* value, brain showed different *f* value from the others regardless of the b values and cardiac gating. 4b gating revealed the best differentiation between the anatomical regions among the three methods. According to the result of 4b gating, parotid gland showed the highest *f* value, followed by submandibular gland, muscle, tonsil and brain. 4b could not show different *f* values between submandibular gland and the other head and neck regions. Muscle and tonsil did not show different *f* values using 4b. 17b showed the poorest differentiation between the anatomical regions. Regarding D value, all anatomical regions showed significantly different values in all three methods. The order of

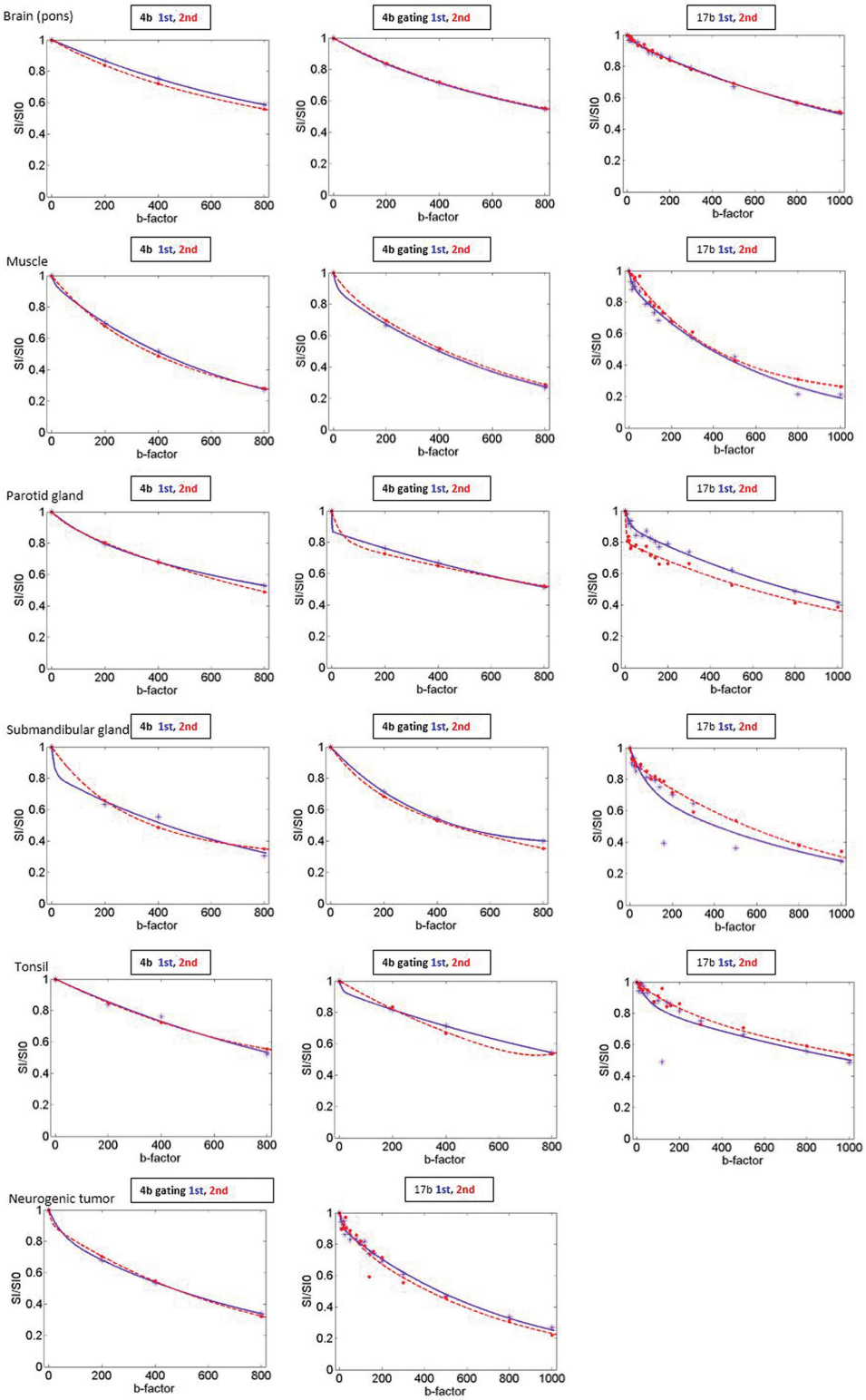

Fig 3. Test-retest fitted curves in the normal head and neck tissues (4b, 4b gating and 17b) in a 50-year-old male volunteer and a neurogenic tumor (4b gating and 17b) in the left level II. The blue dots and line indicate the data points and fitted curves of the 1st exam (test), and the red dots and line indicate the data points and fitted curves of the 2nd exam (retest). In the brain, muscle and submandibular gland, more similar curves being fitted in the test-retest series of 4b gating are noted than those of 4b or 17b. In the parotid gland and tonsil, test-retest fitted curves were not improved using 4b gating compared to 4b. However, in the parotid gland, 4b gating curves show definite hockey – stick appearance which reflects a tendency of higher perfusion fraction of the salivary glands. In 4b series of the parotid gland, the curves are flat. Regarding the tonsils, the shortest sequence, 4b series seem to be the most reliable method because tonsil is susceptible to swallowing motion.

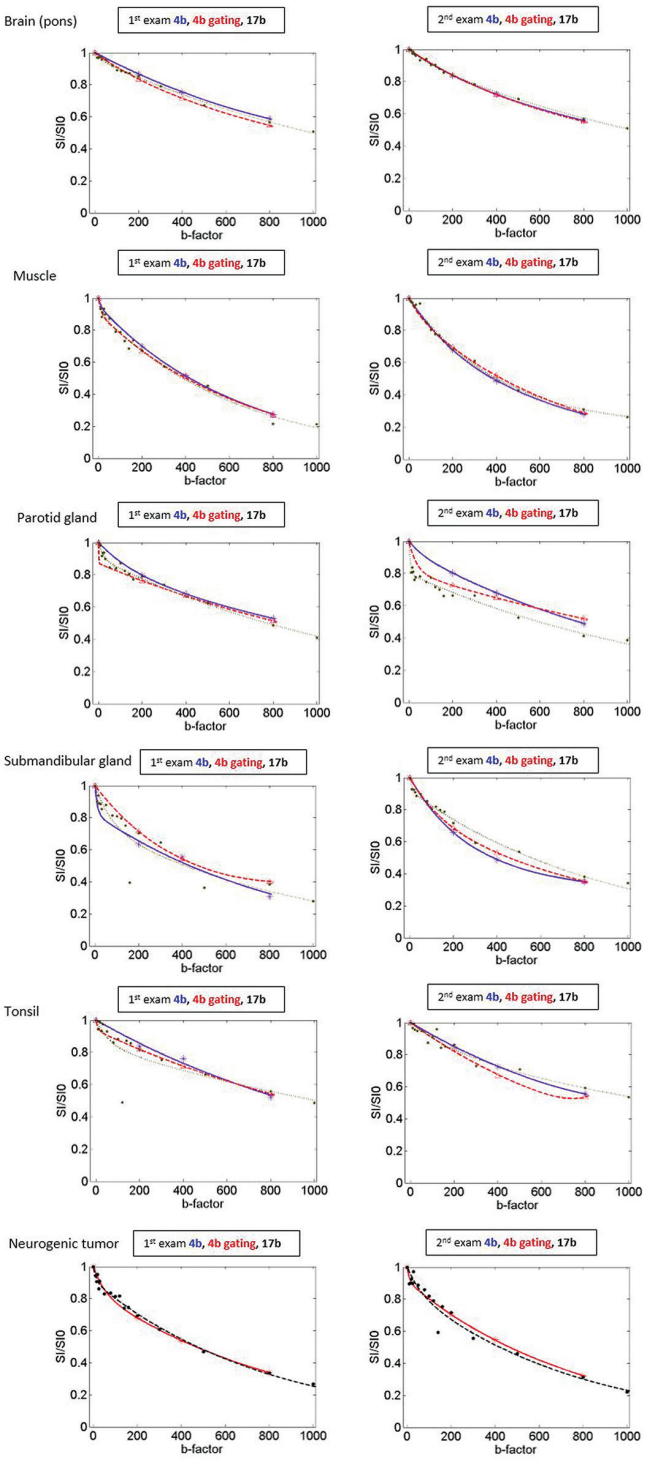

Fig 4. Fitted curves comparing 4b, 4b gating and 17b in the normal head and neck tissues and 4b gating and 17b in a neurogenic tumor in the left level II. The blue, red, black dots and line indicate the data points and fitted curves of 4b, 4b gating and 17b, respectively. Not only the fitted curve of 17b, but also the fitted curves of 4b and 4b gating revealed different shape of biexponential curves according to the perfusion characteristics of the normal tissues and head and neck masses. For example, the fitted curves of the brain and muscle show flattening whereas the fitted curves of the parotid gland and submandibular gland seem to be initially steeper decreased.

D value according the anatomical regions was similar to that of ADC value. D* showed the poorest differentiation between anatomical regions and wide range of the measured values.

Short-term test-retest reproducibility of ADC and IVIM parameters in various head and neck masses

IVIM DWI set with 4b gating and 17b were performed twice in five patients. ROIs were drawn in six masses; one glomus vagale paraganglioma, two bilateral level II metastatic lymph nodes from sinonasal adenocarcinoma and three neurogenic tumors in the posterior paraspinal space, right supraclavicular area and left level II. The size of ROI (mean ± standard deviation) was 217.7 ± 115.1 mm^2.

For all parameters, ICC values were higher using 4b gating than using 17b. For 4b gating, all parameters except D* revealed excellent ICC values (Table 7). All parameters exhibited lower mean CV values using 4b gating than 17b (Table 7). Furthermore, Bland-Altman plot demonstrated narrower 95% limits of agreement between repeated exams for 4b gating than for 17b in all parameters (Table 7). An example of test-retest fitted curve in a neurogenic tumor is in Fig. 3.

The Mann-Whitney test revealed that the values of ADC, *f* and D were not significantly different between 4b gating and 17b ($P = 0.749$ for ADC, $P = 0.873$ for *f*, and $P = 1$ for D, respectively). However, the value of D* was significantly different between 4b gating and 17b ($P = 0.02$). The mean values of repeated measured ADC and IVIM parameters in each mass are described in Table 8. Figure 4 shows fitted curves comparing 4b gating and 17b in a neurogenic tumor.

Discussion

Since the IVIM technique was initially introduced by Le Bihan et al.,[6] it has been used to investigate many regions as a noninvasive technique simultaneously providing both tissue perfusion and diffusion information The head and neck is a difficult region for the application of IVIM DWI because of susceptibility to artifacts around air and bone, and motion artifacts due to swallowing and CSF- or carotid artery-related flow. Therefore, it is important to minimize acquisition time and to reduce the effect of pulsation related flow in the head and neck. In this study, we applied cardiac gating for reproducibility improvement in measurement of IVIM parameters in the head and neck and compared minimum 4b, 4b gating and 17b with respect to short-term test-retest reproducibility.

The present study reported ICC, CV and BAA values for short-term test-retest reproducibility of 4b, 4b gating and 17b. In both normal tissues and various masses in the head and neck, ICC values for ADC, *f* and D from 4b gating were higher than other methods. In addition, all parameters from 4b gating presented lower mean CV using 4b gating and narrower 95% limits of agreement than the methods without cardiac gating in both normal tissues and masses. Although previous studies described the slow diffusion coefficient D did not vary significantly during the cardiac cycle[11,12], because

Table 5. Median values with ranges of measured parameters in the head and neck tissues

		4b	4b gating	17b
Brain	ADC	0.71 (0.53 – 0.78)	0.70 (0.65 – 0.80)	0.67 (0.63 – 0.75)
	f	4.9 (4.1 – 7.7)	5.4 (4.3 – 9.3)	6.2 (3.7 – 8.1)
	D	0.65 (0.61 – 0.74)	0.64 (0.60 – 0.74)	0.63(0.57 – 0.71)
	D*	15.57 (13.32 – 73.23)	15.74 (11.90 – 42.51)	19.83 (12.12 – 48.56)
Muscle	ADC	1.59 (1.49 – – 1.71)	1.57 (1.40 – 1.72)	1.55 (1.43 – 1.66)
	f	10.3 (6.0 – 19.5)	12.25 (7.9 – 26.0)	11.2 (6.4 – 22.6)
	D	1.48 (1.34 – 1.58)	1.45 (1.23 – 1.55)	1.49 (1.30 – 1.62)
	D	26.15 (13.91 – 114.35)	21.31 (14.99 – 45.04)	51.38 (19.43 – 158.05)
Parotid gland	ADC	1.00 (0.84 – 1.21)	0.99 (0.84 – 1.18)	0.92 (0.79 – 1.10)
	f	16.1 (10.2 – 20.3)	15.55 (9.0 – 17.6)	15.0 (9.6 – 26.0)
	D	0.83 (0.71 – 1.05)	0.84 (0.66 – 1.00)	0.84 (0.72 – 0.98)
	D*	22.52 (14.81–61.45)	21.93 (13.96 – 52.55)	52.35 (25.17 – 82.52)
Submandibular glands	ADC	1.17 (0.98 – 1.32)	1.15 (1.05 – 1.29)	1.12 (0.96 – 1.33)
	f	14.3 (8.6 – 22.9)	14.0 (11.0 – 19.3)	15.4 (7.9 – 22.1)
	D	1.00 (0.72 – 1.19)	0.98 (0.89 – 1.13)	1.00 (0.89 – 1.22)
	D*	29.84 (9.58 – 143.29)	20.92 (15.19 – 62.37)	37.66 (3.30 – 102.41)
Tonsil	ADC	0.77 (0.67 – 0.98)	0.75 (0.62 – 0.98)	0.70 (0.60 – 0.95)
	f	12.8 (6.5 – 20.1)	10.5 (6.4 – 14.6)	14.6 (6.2 – 27.9)
	D	0.60 (0.52 – 0.85)	0.62 (0.49 – 0.84)	0.58 (0.40 – 0.84)
	D*	15.54 (8.00 – 29.13)	18.10 (10.66 – 43.25)	46.57 (12.03 – 75.46)

ADC, D, and D* values are expressed as the median value (x10^{-3} mm^2/sec), *f* values are expressed as the median percentage, with ranges in parentheses.

it and perfusion parameters are calculated from the same biexponential equation using the same measured signal intensities and partial volume effects in the voxel level, we believe also diffusion related parameter, D can be more reproducible indirectly by using cardiac gating. Therefore, on the basis of our results, we may suggest that 4b gating was the most reproducible method for IVIM parameters among the three methods.

In contrast to our results, several previous studies regarding b value optimization in the abdominal organs have recommended using at least 8 to 10 b values for accurate estimation of IVIM parameters.[16,25] However, their study designs were different from ours. Previous studies determined optimized b values using Monte Carlo simulations. However, we measured the value of ADC and IVIM parameters on real scans, which were performed with both minimum (i.e., 4b, 4b gating) and sufficient b values (i.e., 17b) and applied cardiac gating to reduce the effect of pulsating flow. Although many concentrations in the low b value have been recommended regarding the estimation of D*[10], our study revealed 17b with sufficient low b values resulted in poorer reproducibility than 4b gating in all parameters including D*. In addition, according to Kruskal-Wallis test, almost all parameters except D* in most normal head and neck tissues exhibited no statistically significant differences between 4b, 4b gating and 17b. Furthermore, the values of ADC, *f* and D from various head and neck masses were not significantly different between 4b gating and 17b. Therefore, the values of ADC, *f* and D acquired using 4b gating seem to represent reproducible quantitative values from biexponential IVIM model.

D* presented the poorest reproducibility and its value was great signal attenuation variability among the acquisitions. Similar to the present findings, several previous studies reported that D* had poor reproducibility in liver metastases, HCC and liver parenchyma.[19,22,26] Because previous studies reported that D* varied significantly according to cardiac cycle,[11,12] we presumed that D* (flow velocity) might be most affected by cardiac cycle, followed by *f* and D and expected to improve the uncertainty of D* using cardiac gating. However, D* maintained poor reproducibility in spite of sufficient low b values and cardiac gating. Although D, D* and *f* were together calculated using the same bi-exponential equation, because D* is much greater than D, the effects of D* on the signal decay at large b values (> 200 sec/mm^2) can be neglected. Therefore, the stability of *f* and D might have influenced each other. Further studies validating the IVIM of D* map should be explored which can reduce misregistration and partial volume effects contributed by bright adjacent vessels.

While cardiac gating could not improve the reproducibility of D*, the other perfusion related factor, *f* value became more reproducible parameter using cardiac gating in both

Table 6. Kruskal-Wallis test with post-hoc analyses to compare ADC and IVIM parameters between the anatomical regions

Parameter		4b	4b gating	17b
ADC	*P* value	< 0.0001	< 0.0001	< 0.0001
	(1) Brain	(2)(3)(4)(5)	(2)(3)(4)(5)	(2)(3)(4)
	(2) Muscle	(1)(3)(4)(5)	(1)(3)(4)(5)	(1)(3)(4)(5)
	(3) Parotid	(1)(2)(4)(5)	(1)(2)(4)(5)	(1)(2)(4)(5)
	(4) Submandibular glands	(1)(2)(3)(5)	(1)(2)(3)(5)	(1)(2)(3)(5)
	(5) Tonsil	(1)(2)(3)(4)	(1)(2)(3)(4)	(2)(3)(4)
f	*P* value	< 0.0001	< 0.0001	< 0.0001
	(1) Brain	(2)(3)(4)(5)	(2)(3)(4)(5)	(2)(3)(4)(5)
	(2) Muscle	(1)(3)	(1)(3)(3)	(1)
	(3) Parotid	(1)(2)(5)	(1)(2)(5)	(1)
	(4) Submandibular glands	(1)	(1)(5)	(1)
	(5) Tonsil	(1)(3)	(1)(2)(3)(4)	(1)
D	*P* value	< 0.0001	< 0.0001	< 0.0001
	(1) Brain	(2)(3)(4)(5)	(2)(3)(4)	(2)(3)(4)(5)
	(2) Muscle	(1)(3)(4)(5)	(1)(3)(4)(5)	(1)(3)(4)(5)
	(3) Parotid	(1)(2)(4)(5)	(1)(2)(4)(5)	(1)(2)(4)(5)
	(4) Submandibular glands	(1)(2)(3)(5)	(1)(2)(3)(5)	(1)(2)(3)(5)
	(5) Tonsil	(1)(2)(3)(4)	(2)(3)(4)	(1)(2)(3)(4)
D*	*P* value	0.0002	0.009	0.0003
	(1) Brain	(2)(4)	(2)(3)(4)(5)	(2)(3)(4)(5)
	(2) Muscle	(1)(5)	(1)	(1)
	(3) Parotid	(5)	(1)	(1)
	(4) Submandibular glands	(1)(5)	(1)	(1)
	(5) Tonsil	(2)(3)(4)	(1)	(1)

Table 7. Short-term test-retest reproducibility of ADC and IVIM parameters in various head and neck lesions

		4b gating	17b
ICC[a]	ADC	0.997 (0.981 – 1)	0.857 (–0.022 – 0.098)
	f	0.986 (0.901 – 0.998)	–0.402 (–9.018 – 0.804)
	D	0.997 (0.978 – 1)	0.813 (–0.334 – 0.974)
	D*	0.664 (–1.400 – 0.953)	0.500 – 0.257 – 0.930)
CV[b]	ADC	3.74	4.49
	f	15.27	22.14
	D	5.67	8.19
	D*	29.24	41.80
BAA[c]	ADC	3.7 (– 2.8, 10.2)	22.0 (–65.1, 109.1)
	f	–1.5 (– 25.3, 22.3)	–19.6 (–216.6, 177.4)
	D	4.5 (– 3.2, 12.2)	24.4 (–64.3, 113.1)
	D*	13.0 (– 76.2, 102.3)	–18.0 (–243.1, 207.1)

All numbers in brackets of [a]ICC indicate the 95% confidence interval. The highest ICC value indicates the best reproducibility. The lowest mean of [b]CV (in %) indicates the best reproducibility. Mean Difference and 95% limits of agreement [c]BAA (in %) are shown. The narrowest value indicates the best reproducibility.

normal tissues and various masses. The *f* has been reported as an important predictor of T-staging of nasopharyngeal carcinomas,[7] therapy monitoring,[4] and prediction of treatment outcomes.[8] Although the *f* values from 4b and 17b was significantly different in the brain, the value of *f* is very low (4.9–6.2%, our study; 4–8%,[27]) in the brain and thus, the IVIM effect is minimal.[16] Not only IVIM parameters but also ADC revealed more reproducible value by applying cardiac gating in both normal tissues and various masses. These results suggest that ADC and IVIM parameters are influenced by pulsating flow. In contrast to IVIM parameters, ADC from 17b presented better ICC, CV value and narrower 95% limits of agreement than those from 4b. While IVIM parameters seem to be more vulnerable to long scan time, ADC value seems more susceptible to the curve fitting than long scan time.

In the subgroup analysis of variable tissues in the head and neck, almost all parameters in the brain, muscle, parotid gland and submandibular glands exhibited the best reproducibility using the 4b gating; they had the lowest CV and narrowest 95% limits of the agreement. In the tonsils, 4b was the most reliable method for almost all parameters. This might be caused by the specific location of the tonsils, which is vulnerable to artifacts related to susceptibility to the air-tissue

Table 8. Mean values of repeated measured ADC and IVIM parameters in the various head and neck lesions

		4b gating	17b
Glomus vagale paraganglioma	ADC	2.47	2.44
	f	12.8	7.51
	D	2.34	2.34
	D*	9.81	12.11
Left metastatic lymph node	ADC	0.99	0.95
	f	9.50	8.15
	D	0.90	0.89
	D*	15.41	19.10
Right metastatic lymph node	ADC	0.89	0.87
	f	13.95	10.05
	D	0.74	0.83
	D*	16.94	77.09
Neurogenic tumor (posterior paraspinal space)	ADC	2.22	1.40
	f	3.41	5.46
	D	2.19	1.36
	D*	14.83	60.83
Neurogenic tumor (supraclavicular area)	ADC	1.60	1.52
	f	9.64	14.80
	D	1.50	1.42
	D*	10.29	39.72
Neurogenic tumor (left level II)	ADC	2.35	2.93
	f	22.30	23.26
	D	2.19	2.48
	D*	7.30	28.03

ADC, D, and D* values are expressed as (x10^{-3} mm^2/sec), and *f* values are expressed as percentage.

interface and swallowing-related motions. Therefore, a short acquisition time seems to be the key to acquiring reliable IVIM DWI in the tonsils.

In the comparison of ADC and IVIM parameters in the different anatomical regions, ADC using 4b and 4b gating and D using 4b and 17b revealed the largest difference. However, regarding *f* value, the most important clinical marker among the parameters,[4,7,8] 4b gating revealed the biggest difference between the anatomical regions followed by 4b. 17b could not show difference in *f* values between the head and neck tissues. It means that 4b gating had significantly different metrics than the 17 b-values protocol (reference standard). Variable tissues in the head and neck had different values from those of the brain. They showed a higher value of ADC and IVIM parameters than those of the brain. Salivary glands (parotid gland and submandibular gland) had a tendency of higher perfusion fraction than muscle and tonsil. Muscle and tonsil revealed different diffusion properties each other. Muscle showed a higher value of diffusion related factors, ADC and D than those of the others. Tonsil had lower values of diffusion related factors than those of the others which reflected high cellularity of the lymphoid tissue. D* could not show consistent and reliable result in all methods.

Determination of the minimal effective b value is crucial for the optimization and validation of IVIM DWI, especially in the head and neck region, which is quite sensitive to motion artifacts. To make IVIM models easier to apply and faster, Sumi et al. introduced a simplified IVIM DWI with three b values (0, 500, 1000 s/mm^2) to provide the perfusion related parameter and D^3. However, the method cannot separate *f* and D*, and the reproducibility has not been validated yet. In addition, their scan time (i.e., 2 minutes 8 seconds) was similar to 4b in our study (i.e., 2 minutes 41 seconds). In a similar acquisition time, application of cardiac gating to minimum four b values allowed the acquisition of ADC and all IVIM parameters with better reproducibility, compared to the values from sufficient b values.

The present study has some limitations. First, the study cohort was small. A larger cohort study containing greater numbers and types of head and neck tumors is needed to validate 4b gating in head and neck masses. Second, the second b value of 200 s/mm^2 seems to be higher compared with the usual recommendation for the evaluation of perfusion effect.[10] Because D* was considered to determine mainly from the signal decay of low b-value which sufficiently include the range of perfusion-related water motion, typically <200 s/mm^2 of b-value, most of D* values from 4b or 4b gating had a tendency underestimation due to the lack of low b-value data. We believe that the inclusion of b value of < 200 s/mm^2 might result in better estimation, which warrants future study. Third, determination of b-value number of four in our study has a limitation. However, according to our results, not only the fitted curve of 17b, but also those of 4b and 4b gating revealed different shape of biexponential curves (flattening or hockey-stick appearance) according to the perfusion characteristics of the normal tissues and head and neck masses (Fig. 4). Although these fitted curves could reflect the different tissue characteristics, most of D* values from 17b had a tendency of higher than the ones from the either of the 4b or 4b gating. We believe that our 4 b-value protocol has a potential to reflect the tissue perfusion as well as diffusion factors. In addition, we could observe more difference between test-retest fitted curve in 17b than in 4b or 4b gating (Fig. 3). Fourth, we surveyed previous studies which applied IVIM imaging in the head and neck and found that 17b value was the highest number of the b-value among them, which seems to be sufficient b-value scan. In addition, in theory, we believe that 4 b-value protocol can minimally be obtained with the shortest scan time. It could be possible to reduce the scan time by decreasing NEX or voxel size. However, the studies were performed on the 1.5T MRI and based on the EPI sequence which used bandwidth of 250 kHz, so it had insufficient SNR for the experiment. Therefore, we planned to test the advantage of cardiac gating added on the IVIM imaging with the

shortest acquisition time, which was compared to the protocol with sufficient 17 b-values. Fifth, to improve the reproducibility of IVIM imaging, we focused on reducing acquisition time and cardiac gating. Although some attempts to reduce the susceptibility artifact could be considered in the head and neck area (e.g. multi-shot EPI, RESOLVE, turbo spin echo-DWI, and zoom DWI etc.), we did not apply those techniques in this study because they definitely lead to the prolongation of scan time.

All statistical analyses in our study revealed consistently excellent reproducibility with 4b gating. Therefore, the cardiac gated acquisition is more stable than the non-gated ones in our study. One paradox is that cardiac gated values are more reliably repeated does not mean that IVIM parameters are inherently dependent on the flow. Bulk flow is suppressed by the diffusion gradients. However, as previous studies reported that the cardiac gating seemed to affect ADC and IVIM parameters in the brain and kidney,[11,12] it seems that the pulsation affects somewhat the repeatability of the values in the head and neck.

Conclusion

In conclusion, we were able to assess short-term test-retest reproducibility of ADC and IVIM parameters using 4b, 4b gating and 17b in normal head and neck tissues. IVIM DWI using 4b gating was more reproducible for the measurement of IVIM parameters in the various head and neck tissues and masses than imaging with 4b or 17b.

Funding

This study was supported by the Korea Healthcare technology R&D Projects, Ministry for Health, Welfare & Family Affairs (HI13C0015) and by the Research Center Program of IBS (Institute for Basic Science) and by the Convergence Research Program from School of Dentistry and College of Medicine, and Seoul National University (800-20130490) in Korea.

Conflicts of Interest

The authors declare that they have no conflicts of interest.

References

1. Zhang SX, Jia Qj, Zhang ZP, et al. Intravoxel incoherent motion MRI: emerging applications for nasopharyngeal carcinoma at the primary site. Eur Radiol 2014;24:1998–2004.
2. Marzi S, Forina C, Marucci L, et al. Early radiation-induced changes evaluated by intravoxel incoherent motion in the major salivary glands. J Magn Reson Imaging 2015; 41:974–982.
3. Sumi M, Nakamura T. Head and neck tumors: assessment of perfusion-related parameters and diffusion coefficients based on the intravoxel incoherent motion model. AJNR Am J Neuroradiol 2013;34:410–416.
4. Hauser T, Essig M, Jensen A, et al. Characterization and therapy monitoring of head and neck carcinomas using diffusion-imaging-based intravoxel incoherent motion parameters-preliminary results. Neuroradiology 2013; 55: 527–536.
5. Sumi M, Van Cauteren M, Sumi T, Obara M, Ichikawa Y, Nakamura T. Salivary gland tumors: use of intravoxel incoherent motion MR imaging for assessment of diffusion and perfusion for the differentiation of benign from malignant tumors. Radiology 2012; 263:770–777.
6. Le Bihan D, Breton E, Lallemand D, Aubin M, Vignaud J, Laval-Jeantet M. Separation of diffusion and perfusion in intravoxel incoherent motion MR imaging. Radiology 1988; 168:497–505.
7. Lai V, Li X, Lee VHF, et al. Nasopharyngeal carcinoma: comparison of diffusion and perfusion characteristics between different tumour stages using intravoxel incoherent motion MR imaging. Eur Radiol 2014; 24:176–183.
8. Hauser T, Essig M, Jensen A, et al. Prediction of treatment response in head and neck carcinomas using IVIM-DWI: Evaluation of lymph node metastasis. Eur J Radiol 2014; 83:783–787.
9. Le Bihan D, Turner R, Douek P, Patronas N. Diffusion MR imaging: clinical applications. AJR Am J Roentgenol 1992; 159: 591–599.
10. Koh DM, Collins DJ, Orton MR. Intravoxel incoherent motion in body diffusion-weighted MRI: reality and challenges. AJR Am J Roentgenol 2011; 196:1351–1361.
11. Wittsack HJ, Lanzman RS, Quentin M, et al. Temporally resolved electrocardiogram-triggered diffusion-weighted imaging of the human kidney: correlation between intravoxel incoherent motion parameters and renal blood flow at different time points of the cardiac cycle. Invest Radiol 2012; 47:226–230.
12. Federau C, Hagmann P, Maeder P, et al. Dependence of brain intravoxel incoherent motion perfusion parameters on the cardiac cycle. PloS one 2013; 8:e72856.
13. Wetscherek A, Stieltjes B, Laun FB. Flow-compensated intravoxel incoherent motion diffusion imaging. Magn Reson Med 2015; 74:410–419.
14. Tymofiyeva O, Vaegler S, Rottner K, et al. Influence of dental materials on dental MRI. Dentomaxillofac Radiol 2013; 42:20120271.
15. Luciani A, Vignaud A, Cavet M, et al. Liver cirrhosis: intravoxel incoherent motion MR imaging—pilot study 1. Radiology 2008; 249:891–899.
16. Lemke A, Stieltjes B, Schad LR, Laun FB. Toward an optimal distribution of b values for intravoxel incoherent motion imaging. Magn Reson Imaging 2011; 29:766–776.
17. Zhang JL, Sigmund EE, Rusinek H, et al. Optimization of b-value sampling for diffusion-weighted imaging of the kidney. Magn Reson Med 2012; 67:89–97.
18. Chen X, Qin L, Pan D, et al. Liver diffusion-weighted mr imaging: reproducibility comparison of ADC measurements obtained with multiple breath-hold, free-breathing, respiratory-triggered, and navigator-triggered techniques. Radiology 2014; 271:113–125.
19. Kakite S, Dyvorne H, Besa C, et al. Hepatocellular carcinoma: Short-term reproducibility of apparent diffusion coefficient

and intravoxel incoherent motion parameters at 3.0 T. J Magn Reson Imaging 2015; 41:149–156.
20. Jung SC, Choi SH, Yeom JA, et al. Cerebral blood volume analysis in glioblastomas using dynamic susceptibility contrast-enhanced perfusion MRI: a comparison of manual and semiautomatic segmentation methods. PloS one 2013; 8:e69323.
21. Gaens ME, Backes WH, Rozel S, et al. Dynamic contrast-enhanced MR imaging of carotid atherosclerotic plaque: model selection, reproducibility, and validation. Radiology 2013; 266:271–279.
22. Dyvorne HA, Galea N, Nevers T, et al. Diffusion-weighted imaging of the liver with multiple b values: effect of diffusion gradient polarity and breathing acquisition on image quality and intravoxel incoherent motion parameters—a pilot study. Radiology 2013; 266:920–929.
23. Kang KM, Lee JM, Yoon JH, Kiefer B, Han JK, Choi BI. Intravoxel incoherent motion diffusion-weighted MR imaging for characterization of focal pancreatic lesions. Radiology 2014; 270:444–453.
24. Reed GF, Lynn F, Meade BD. Use of coefficient of variation in assessing variability of quantitative assays. Clin Diagn Lab Immunol 2002; 9:1235–1239.
25. Jambor I, Merisaari H, Aronen HJ, et al. Optimization of b-value distribution for biexponential diffusion-weighted MR imaging of normal prostate. J Magn Reson Imaging 2014; 39:1213–1222.
26. Andreou A, Koh D, Collins D, et al. Measurement reproducibility of perfusion fraction and pseudodiffusion coefficient derived by intravoxel incoherent motion diffusion-weighted MR imaging in normal liver and metastases. Eur Radiol 2013; 23:428–434.
27. Federau C, O'Brien K, Meuli R, Hagmann P, Maeder P. Measuring brain perfusion with intravoxel incoherent motion (IVIM): initial clinical experience. J Magn Reson Imaging 2014; 39:624–632.